IEEE Access
Multidisciplinary | Rapid Review | Open Access Journal

Received September 28, 2017, accepted October 31, 2017, date of publication November 8, 2017, date of current version December 5, 2017.

Digital Object Identifier 10.1109/ACCESS.2017.2771310

Review of Application of the Electrical Structure in Resistance Spot Welding

KANG ZHOU[1] AND PING YAO[2,3]

[1]State Key Laboratory of High-Temperature Gas Dynamics, Institute of Mechanics, Chinese Academy of Sciences, Beijing 100190, China
[2]College of Electromechanical Engineering, Guangdong Polytechnic Normal University, Guangzhou 510635, China
[3]School of Mechanical and Automotive Engineering, South China University of Technology, Guangzhou 510640, China

Corresponding author: Ping Yao (ypsunny@163.com)

This work was supported in part by the Natural Science Foundation of China under Grant 51605103, in part by the Characteristic Innovation Project of Guangdong Province Ordinary University under Grant 2014KTSCX145, in part by the Natural Science Foundation of Guangdong Province under Grant 2015A030313663, and in part by the China Postdoctoral Science Foundation under Grant 2016M602461.

ABSTRACT Resistance spot welding (RSW) is frequently employed in current industrial occasions. This paper reviewed recent advances of the electrical structure of the RSW system. Two types of electrical structures are used in RSW machines. Single-phase ac power source has a simple structure but low control frequency and power factor, and the measurement and control for the machine have some special operations. While three-phase medium frequency dc power source has a complex structure and high control frequency but high cost, and frequently switching the direction of the output welding current may induce many negative phenomena in the welding transformer. The characteristics of the two structures are presented in detail in this paper. Corresponding measures have been taken to deal with the phenomena during the process, respectively, for the two types of electrical structures, according to the previous works. Though many significant achievements have been gained in previous works, it is expected to be more improvements required in the future. This paper can provide references and enlightens for academic researches or actual production in RSW operations.

INDEX TERMS Resistance spot welding (RSW), signal-phase ac, three-phase medium frequency dc, welding current.

I. INTRODUCTION

Resistance spot welding (RSW) is one of the most commonly employed process in modern manufacturing industry, especially in automobile production [1]–[3]. The vehicle components, which includes the body in white, cradles, doors, are made of thin metal sheets that are connected using RSW joints. Despite the fact that many advanced spot welding technologies, such as gas tungsten arc spot, laser spot or friction stir spot, are available, the conventional RSW is the predominant process in sheet metal joining particular in automobile manufacturing occasions [4]. Currently, over 90% of assembly work in a car body is completed by RSW [5]. Hence, it is a vital joining process for automobile production.

During the RSW process, two or more parent sheet metals are pressed through upper electrode moving toward to the lower electrode by means of the electrode force, which is usually provided by air pressure in a pneumatic cylinder, or servo actuator. Then the external energy can be delivered into the system through a particular electrical structure and a step-down welding transformer. When the welding current goes through the contact metal sheets, the energy generates following the basic Joule heat generation equation:

$$E = \int_{T_1}^{T_2} I^2(t)R(t)dt, \tag{1}$$

There are two types of electrical sources of the RSW machine responsible for controlling the energy delivery into the welding system: single-phase AC power source and three-phase medium frequency DC power source. Both of two sources are prevalently employed in reality. They have different working principle and can generate different effects during the process [6]–[8]. In single-phase AC power source, two silicon controlled rectifiers (SCRs), also names as thyristors, are connected in parallel: one to pass the current during the positive half cycle and the other during the negative half cycle [9], [10].

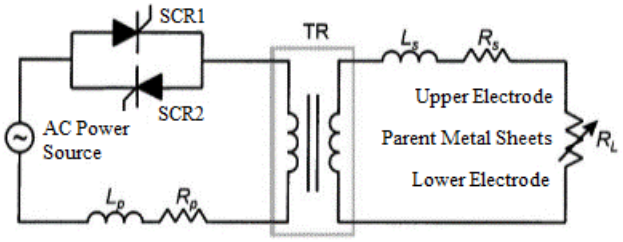

FIGURE 1. Structure of the single-phase AC power source for RSW.

Figure.1 shows the structure of the single-phase AC power source.

In Figure.1, *TR* denotes the welding transformer, which is a typical step-down transformer, and L_p and R_p denote respectively the equivalent inductive reactance and resistance in the primary coil of the transformer, while the L_s and R_s respectively denote the equivalent items in the secondary coil. In this structure, the welding control action is conducted through setting the firing angle, also named as trigger time, of each SCR alternatively for each control cycle. The value range [0, 180°] of firing angle linearly corresponds to the value range [0, 10ms] of firing angle, the transformation is based on the frequency of AC power, which is 50Hz or 60Hz. In other words, the value of firing angle determines the amount of energy delivered into the welding system. The welding operation is conducted between the trigger time of the SCR and the next zero crossing of the welding current, and the duration is called as conduction time, which can also correspond to a conduction angle. Under the circumstance, the working frequency is twice of the frequency of AC power source, and the welding heating process is not successive and each burst of pulsed current passed through the parent metal sheets followed by an idle time. Though it has a low cost and easy-manipulating structure, the efficiency is not very high in reality.

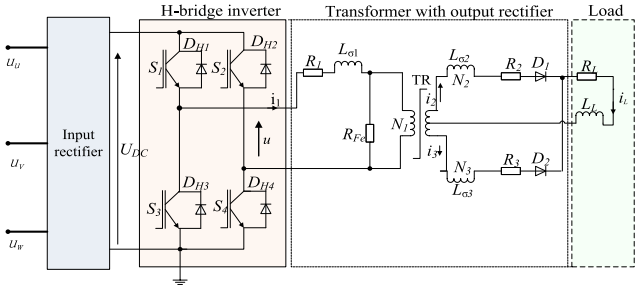

FIGURE 2. Structure of the three-phase medium-frequency DC power source for RSW.

On the other hand, other type of power source is the three-phase medium frequency DC power source. It employs a three-phase AC power source, an input rectifier, an H-bridge inverter, and a welding transformer, and other auxiliary equipment, the structure can be shown in Figure.2. In Figure.2, *TR* is also a step-down welding transformer, u_u, u_v, u_w are three phase AC power source from common electrical grid, the input rectifier, which is a three-phase full-wave rectifier, can output an approximate DC voltage U_{DC}. The square voltage u, which is a voltage in the primary coil of the welding current, is an output of the H-bridge, which is composed of four IGBT (Insulated Gate Bipolar Transistor) transistors S_1 to S_4 and corresponding diodes $D_{H1} \sim D_{H4}$. It can be seen that the output voltage of the inverter is either U_{DC} when the transistors S_1 and S_4 are switched on, or $-U_{DC}$ when the transistors S_2 and S_3 are switched on, and the load voltage is 0 when all of four transistors are switched off. The statues of IGBTs are controlled by a separated PWM (Pulse Width Modulation) controller. The control variable is the duty cycle of the PWM wave. In other words, the input rectifier transforms the original three-phase AC voltage to approximate DC voltage, and then the H-bridge transforms it to square wave AC voltage to suitable for the welding transformer. The welding transformer includes one primary coil and two secondary coils, whose numbers of turns are N_1, N_2 and N_3, and i_1, i_2 and i_3 are corresponding currents in the coils, while $R_1 \sim R_3$ and $L_{\sigma 1} \sim L_{\sigma 3}$ are corresponding equivalent resistances and leak inductances in the corresponding coils. The R_{Fe} is the iron core losses of the welding transformer *TR*, which are connected to output rectifier diode D_1 and D_2, while R_L and L_L denote the loads. In this structure, the working frequency can be adjusted to be a very high value, in general, at 500∼20000Hz. Compared to the single-phase AC power source, the welding operation process is successive because the welding current can go thought the parent metal sheets all the time during the process. In addition, higher frequency denotes more control actions can be employed to adjust the energy delivery in reality. Hence, it has higher efficiency than that of single-phase AC power source.

Currently, both two power sources are employed in practical occasions. Single-phase AC power source RSW machine is predominantly employed in automotive industry. The three-phase medium frequency DC power source RSW machine has been limited to more specialized applications, such as the seam welding and aluminum welding in the aerospace industry, where the high power need often requires the use of three-phase rectifier welding current [6]. It can save energy and have larger range of appropriate welding conditions, however, it has higher cost and more complex structure than that of AC power source [6], [11], [12]. Recently, as the technology developing, two structures may also be used in some occasions which usually employed other structure. For example, the medium frequency DC power source can also be utilized in automotive manufacturing. Though the RSW has some other different structures, such as single-side structure [13]–[15], or has different processes for different types of parent metal sheets, such as small scale RSW and large scale RSW processes [16], [17], the two types of power sources were applied in all of the RSW machines.

According to above introduction, the control system of RSW machines is single-input-single-output (SISO) control

system, the sole input is the firing angle of the SCR in the single-phase AC RSW machine, or duty cycle of the PWM wave in the three-phase medium frequency DC RSW machine, respectively. While the output is the welding current, or other types of energy delivery. Hence, it is a highly nonlinear system, also, because the load resistance is varying during the welding process, it is also a time-varying system. Therefore, the characteristics of the electrical structure should be seriously considered during the academic research and actual production process.

Electrical system is the executive structure of the RSW machine, however, fewer previous works focused on the electrical structure of the RSW machine, compared to the other aspects of works in the RSW relative area. Currently, microcontroller was employed widely in RSW system design and actual production [18], [19]. The electrical structure, which conducted the external energy delivery into the RSW system, should be considered seriously in the work, because it related to the stability, safety and energy efficiency of the production, then to facilitate the micro-controller system. In this paper, only the works of the energy delivery concerning electrical structure is involved, and the effect of measuring and controlling actions on the weld quality will be not included. In addition, because two types of RSW machines have different electrical structures and working principles, the works related to the two types will be separately reviewed in this work.

In this paper, some recent contributions and advances related to the electrical structure of the RSW machine will be reviewed. Section.2 will focus on the works related to the single-phase AC RSW power source, while section.3 will consider the relative works dealing with the medium frequency DC RSW power source. Section.4 will be the concluding remarks and suggestion for the future works.

II. SINGLE-PHASE AC RSW MACHINE

For single-phase AC RSW machine, the control action is to set the firing angle of the SCR during each control cycle. Figure.3 shows an integrated waveform in one control cycle and a successive waveform of electrode force and welding current.

In Figure.3, α denotes the firing angle of the corresponding SCR, θ is the conduction angle which denotes the effective range of welding current, because the existence of inductive components, the output voltage and current in the second coil of the welding transformer have a phase difference, ψ is the corresponding phase lag angle. In Figure.4 (a), there are two vertical axis P and S, which respectively denote the beginning of voltage in the primary coil and output welding current in the second coil, φ is the power factor angle which denotes the phase difference between input voltage and corresponding current, its mathematical description is $\varphi = \arctan(\omega L/R)$, where L and R respectively denote the equivalent inductance and resistance, their equivalent reactance is Z, which description is $Z = \sqrt{R^2 + (\omega L)^2}$ and ω is the angle frequency, the description is $\omega = 2\pi f$. In addition, γ denotes the

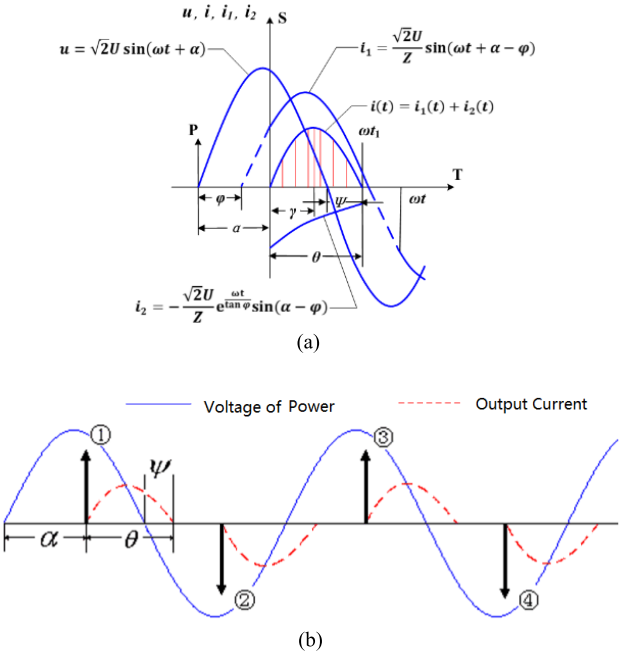

FIGURE 3. Electrical waveform of single-phase AC power source (a). Integrated waveform in one control cycle (b).Successive waveform of voltage and current [20].

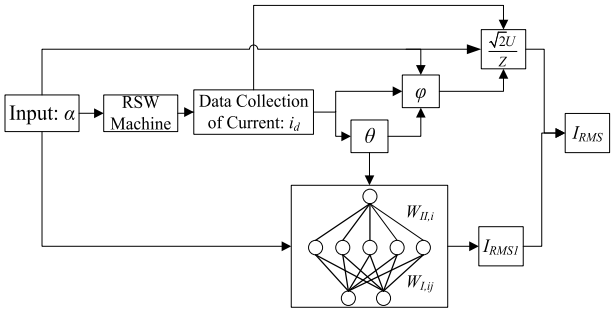

FIGURE 4. Block diagram of the RMS value of welding current calculation process [29].

angle which corresponds to the peak of the welding current. It can be seen that the value of α determines the amount of energy delivered into the welding system, and corresponding the values of output electrode voltage and welding current. In other words, all of the currents in the primary and secondary coils are depended by the SCR firing angle input α in the primary coil [21]. Smaller value of α, larger electrode voltage and welding current will be outputted.

According to Figure.3, the actual welding current is not successive in reality, and if the firing angle is properly set, the actual welding current may be successive because the current in the next control cycle begins at the termination of the current in the preceding control cycle, and this phenomenon is called full-conduction and denotes that the maximum capacity of the RSW machine were used, under this circumstance, $\alpha = \varphi$ and $\theta = 180°$. However, if the firing angle α is below

the power factor angle φ, the corresponding SCR cannot be triggered even though the pulse signal comes because the voltage of SCR is opposite to the coming pulse signal. If successive control cycles cannot be alternatively triggered, the magnetic saturation of the welding transformer may appear, which may damage the circuit or SCR. In addition, when α is equal to φ, the system achieves critical stable, and when α is larger than φ, the system is stable and it is a common used situation. Our previous work [22] analyzed three situations in detail and proposed a solution to assure the stable trigger for each cycle. The work analyzed the relation between firing angle α, conduction angle θ and power factor angle φ, and found that the mathematical relation can be written as:

$$\sin(\theta + \alpha - \varphi) - \sin(\alpha - \varphi)e^{\frac{-\theta}{\tan\varphi}} = 0. \tag{2}$$

This is a transcendental equation and the power factor φ cannot be directly obtained according to known α and θ. However, after plotted the figure, the relation can be approximately described as a line equation as follows:

$$\varphi = \pi[1 - (\pi - \alpha)/\theta]. \tag{3}$$

This equation can approximately obtain the power factor φ. Hence, for each next control cycle, the actual α may be above the value of φ calculated in the preceding control cycle. Though the approximation included errors, the errors made the firing angle α bigger. Then a safety trigger can be obtained.

Apart from the safety trigger, the unknown power factor may induce some other problems. Hence, some previous works devoted to online calculating the power factor. Gong *et al.* [23] obtained a mathematical relation which showed that the power factor λ can only be relative to the firing angle α and current peak angle γ, and then employed an error back propagation (EBP) network to obtain the power factor according to the two inputs. The network included two hidden layers containing respectively 20 and 30 neural nodes, and employed to form a $2\times20\times30\times1$ network topology architecture. However, the structure is so complex and the online calculation may consume large amount of CPU time, and the original data is collected with 5° interval, which may induce large errors in final results. Also, our previous work [10] tried to solve the same problem. In the work, a direct integral method was employed, then an analytical mathematical description can be obtained in equation (4), as shown at the bottom of this page.

The equation used two different conduction angles, one was the whole conduction angle in one control cycle and the other was the conduction range from the zero point of welding current to the peak. They were respectively denoted as θ and θ_1. Moreover, T_s was the discrete sample cycle, and M and N respectively denoted the sampling number corresponding the ranges of θ and θ_1, i_d was the discrete sampling value of welding current. According to the comparison between calculated results and ideal reference, which was obtained from numerical calculation for power factor angle based on equation (2) using MATLAB, the calculation of φ was reliable. Then combined definition of power factor, the overall value of power factor can be correspondingly obtained. After making comparison between reference and actual calculating value, the maximum error was below 10% when different firing angles were employed.

In addition, during the single-phase AC RSW operation process, the voltage seriously fluctuates between positive value, zero and negative value, in other words, large voltage fluctuations appeared in the system, and serious voltage flicker was caused by frequent and rapid operating characteristics of the machine. The process generated large number of reactive power demand and harmonic current waveform distortion. The high-reactance welding transformer can induce low-power-factor loads. A welding factory may employ hundreds of welding machines, the synchronized welding cycles may lead to annoying flickers. Severe voltage variations can reduce the power delivered to the welding system and cause reduced heat energy and poor-quality welding products. To overcome this shortcoming, a mini-static var compensator (SVC) was designed and applied to compensate voltage unbalance caused by single-phase low-power-factor loads, and improve the voltage quality on the welding circuit of industrial power distribution system [24]. The rating of an SVC is determined by the specific system requirement and desired performance. Its size depends on some basic factors: short-circuit capacity of the system at the load bus, voltage drop to be compensated, and the range of welding load. Equation (2) can be employed to calculate the additional reactive power required to increase the voltage. The design was anticipated to be an attractive methods of dealing with flicker, voltage dips, and reactive power problem on low-voltage network. Also, Ko and Gu [25] proposed a thyristor switched capacity (TSC) bank to improve the voltage flicker. The proposed TSC can compensate the power factor and implement rapid compensate to meet the fast changing characteristics of the machine. Final experimental results showed the actual voltage fluctuation and total harmonic voltage distortion were effectively reduced.

Currently, majority of welding actions use welding current as the control variable, and the root-mean-square (RMS) value of welding current is commonly employed as the calculating and measuring criterion [26]. Hence, the accurate

$$\varphi = \arctan\{2\pi f \cdot T_s \frac{[\cos\alpha - \cos(\alpha + \theta_1)] \cdot \sum_{j=1}^{N} i_d(j) - [\cos\alpha - \cos(\alpha + \theta)] \cdot \sum_{j=1}^{M} i_d(j)}{i\big|_{\omega t=\theta_1} \cdot [\cos\alpha - \cos(\alpha + \theta)]}\}. \tag{4}$$

measurement of RMS value of welding current is very important. Traditional successive integration from point to point for all collected current data based on the definition of RSW value:

$$I_{RMS} = \sqrt{\frac{1}{T}\int_0^T i^2(t)dt}. \tag{5}$$

where I_{RMS} is the RMS value of the welding current, T is the duration of welding current passing through the parent metal sheets, the range corresponds to the conduction angle θ. Then for the actual welding system, the discrete format is as follows:

$$I_{RMS(d)} = \sqrt{\frac{1}{N}\sum_{I=0}^{N} i_d^2}. \tag{6}$$

where $I_{RMS(d)}$ is the discrete format of the RMS value, N is the number of sampling during one control cycle, i_d is the corresponding discrete sampling value. However, this traditional method may consume more CPU time in reality. Some early works [27], [28] tried to find the relations between RMS value of welding current and peak value, or current zero-crossing derivative, and then employed specific mathematical tools, such as statistical analysis, or neural network to obtain the RMS value of welding current. However, because the mathematical models were relative to the concrete experimental process and have complicate formats, they can only be used in some simple and limited occasions. In our previous work [29], we tried to study the mathematical model of the single-phase AC RSW model, and divided the mathematical description into two parts: one was model-dependent part which was relative to peak of the welding current and power factor angle φ, the other is model-independent part which was only relative to α, θ and φ. The former part can be obtained based on equation (4) and measured peak of welding current, while the later part can be modelled using neural network. Because the later part was only relative the numerical relation between three angles, the established model was model-independent and can be used in other circuits with the similar structures, in other word, it was a general model and irrelative to a concrete experiment. The block diagram can be shown in Figure.4 [29].

In Figure.4, $\sqrt{2}U/Z$ denoted the model-dependent part, and I_{RMS1} was the model-independent part which was calculated by a neural network, and then the I_{RMS} can be obtained by combining the two parts. The experimental results showed that the method can save about 40% of the CPU time with small calculation errors.

Then for control operation of single-phase AC RSW machine, a lot of previous works considered it. The percent of the energy is commonly used in some academic contributions, or actual industrial operation [30]. It considers the full-conduction, which the actual welding current shown in Figure.4 (b) is successive and no idle exists between two welding currents, as the 100% energy delivery, and then makes the required percent of energy corresponding to a specific fire angle in reality. The mathematical description of the relation can be shown. I_a denotes the current value when firing angle is α, I_f denotes the current value when full-conduction appears and $\alpha = \varphi$, as well as $\theta = 180°$, hence, the current percentage is $I\% = I_a/I_f$, then for a concrete welding operation, the firing angle α can be written as:

$$\alpha = f(I\%). \tag{7}$$

The detailed mathematical relation is highly nonlinear, it can be shown as follows [31]:

$$\begin{cases} I_f = [\frac{1}{\pi}\int_0^{\pi}(\sqrt{2}U\sin\omega t/R)^2 d(\omega t)]^{\frac{1}{2}} \\ \qquad\qquad \Rightarrow 2\pi(1 - I\%^2) = 2\alpha - \sin(2\alpha). \\ I_\alpha = [\frac{1}{\pi}\int_\alpha^{\pi}(\sqrt{2}U\sin\omega t/R)^2 d(\omega t)]^{\frac{1}{2}} \end{cases} \tag{8}$$

In most academic experiments research, accurate control operation is necessary. Generally, constant current control (CCC) method is a commonly-employed control strategy, because of its simplicity, reliability and performance [32], as well as the liquid nugget can steadily grow under the control mode [33]. To achieve the CCC, the relation between fringe angle α and the desired welding current should be established. The relation is also highly nonlinear. The difficulties for achieving the goal are that the welding load is varying and the electrical grid may be fluctuated, especially when many machines synchronously work. In previous works, Zhao and Cai [34] proposed a controller which combined Flourier learning and PD controller. Its block diagram is shown in Figure.5 [34].

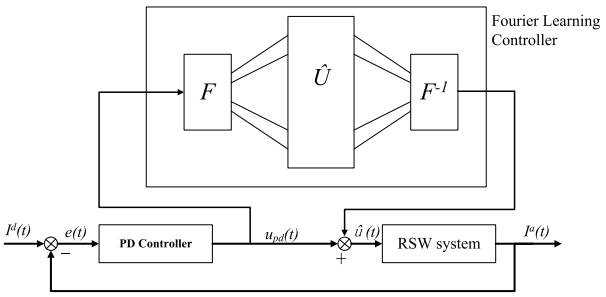

FIGURE 5. Block diagram of the controller combined Flourier learning and PD controller [34].

The controller was model-irrelative, and the learning part generated feedback compensation based on the Flourier approximation of the PD controller. Though there were other approximate works to deal with the CCC, the algorithm did not consider the structure and working principle of the circuit, they were not general. In our previous work [20], the working principle and relations between different variables were seriously analyzed, and then a nonlinear relation between desired welding current I_R^d and firing angle α based on the actual welding current $I_{R,i}^a$ in current control cycle can be obtained as in (9), as shown at the top of the next page, where i is the actual control cycle. In addition, because the

$$\alpha_{i+1} = \frac{\arccos[\frac{I_R^d}{I_{R,i}^a} \cdot [\cos(0.1\pi\alpha_i) - \cos[0.1\pi(10+\psi_i)]] + \cos[0.1\pi(10+\psi_i)]]}{(0.1\pi)}. \tag{9}$$

$$\hat{\alpha}_{i+1} = \frac{\arccos[\sqrt{\frac{E_R^d}{E_{R,i}^a} \cdot \frac{\hat{R}^d}{R_{i-1}^a}} \cdot [\cos(0.1\pi\bar{\alpha}_i) - \cos[0.1\pi(10+\psi_i)]] + \cos[0.1\pi(10+\psi_i)]]}{(0.1\pi)}. \tag{11}$$

positive trigger and negative trigger for two SCRs may have difference, or cycles of Analog-Digital (AD) data acquisition may have errors, a PD controller was employed to alleviate the fluctuation of two triggers, and the PD controller was not traditional because the input and output have the same units, hence, the parameters of the controller was easy to be confirmed and no large fluctuation appeared. The PD controller can be written in following format:

$$\bar{\alpha}_{i+1} = \bar{\alpha}_i + K_p(\hat{\alpha}_{i+1} - \bar{\alpha}_i) + K_d[(\hat{\alpha}_{i+1} - \bar{\alpha}_i) - (\hat{\alpha}_i - \bar{\alpha}_{i-1})], \tag{10}$$

where $\bar{\alpha}$ was the actual trigger time for the controller, K_p and K_d were the feedback gains, while $\hat{\alpha}$ corresponded to the result of equation (9). The experimental results showed that the controller can achieve the goal of CCC when different desired welding currents were set. Because the controller was designed based on electrical structure and working principle of the RSW system, the controller was irrelative to the concrete welding process and can be universal in all of the single-phase AC RSW operation. In addition, because the model was based on characteristics of electrical structure, it can be extended to be employed in other kinds of control, for example, constant energy control (CEC), which also was named as constant power control (CPC). Our other work [35] have realized the CEC based on CCC, equation (11), can be written based on the relation between desired energy and firing angle in equation (11), as shown at the top of this page, where E_R^d was the desired energy, $E_{R,i}^a$ was the actual energy in current control cycle. The equation transformation was based on equation (1). The calculation of energy was relative to the dynamic resistance R, because the desired value of dynamic resistance in the next control cycle was unknown, the mean value of dynamic resistance during two adjacent control cycles can be used as a substitute, whose mathematic description can be $\hat{R}^d = (R(i) + R(i-1))/2$, also, R^a was the actual dynamic resistance in the specific control cycles.

As the most commonly used type of power source, many important measurements should concern the characteristics of single-phase AC RSW machine. As one of the most commonly-employed process variable, dynamic resistance was used in online process analysis, non-destructive quality test, and other relative occasions, because it can be related to weld strength during the process [36]. Though the dynamic resistance can be obtained by electrode voltage and welding current, directly calculation may induce disaster results because the so many noises exist in the signals. Moreover, the two values are collected by different sensors, the voltage detector collects the electrode voltage and the Rogowski current transducer collected the welding current signals, and result from Rogowski current transducer must be processed by circuit or algorithm design. Hence, the two values may not be one-to-one correspondence. The electrode voltage included the inductive elements and resistance elements, which shows [37], [38]:

$$V = iR + L\frac{di}{dt}. \tag{12}$$

where V, i, R, L respectively denote the electrode voltage, welding current, dynamic resistance, equivalent inductive between electrodes. These values are collected between two electrodes and in the secondary coil of the welding transformer. Traditionally, two methods were used to online calculate the dynamic resistance. The first method was using the instantaneous electrode voltage at the peak of the welding current during each cycle dividing the corresponding welding current, because at that point, the differential value of the welding current is zero and the inductive element can be eliminated. Following the same principle, Cho and Rhee [39], [40] obtained the dynamic resistance in the primary coil of the welding transformer to avoid add some facilities in the second coil. The second method was based on the calculation of RMS values of electrode voltage and welding current [41]. However, using these two methods, only one value can be obtained during each welding cycle. It may be limited in some detailed analysis by means of dynamic resistance. To solve this problem, some previous works employed a special data acquisition unit [42] or a signal conditioning board with a tuning potentiometer [11]. However, the facility was so complex and increase the cost. In our previous work [33], the historical information was used to eliminate the noises and disturbances during the calculation as shown in equation(13):

$$R = \frac{\sum_{\text{two continuous cycles:}} U(t)I(t)}{\sum_{\text{two continuous cycles:}} I^2(t)}. \tag{13}$$

Using this method, dynamic resistance with high frequency can be obtained. The frequency was same as that of data collection frequency. Final results showed that variation of the dynamic resistance was similar to that obtained using RMS values, but with high frequency.

Actually, single-phase AC RSW power source is used more in current RSW occasions. However, the particular

structure makes some operation difficulty, such as power factor measurement, stable welding energy or current output, or dynamic resistance measurement, and so on. To solve these problems to serve the welding operation, the characteristics of electrical structure must be clearly understood, and then make appropriate designs. The previous works seriously considered the power source and obtained some significant achievement. However, the accuracy of the measurement and control is related to the features of the circuit, which is alternatively triggered by positive and negative signals, the tiny difference may induce large errors because of existence of the welding transformer. In addition, the control action must be taken in each trigger, and this low frequency control cannot avoid possible large disturbances in the system. Hence, the system is expected to be further improved and then achieve to be higher accuracy in the future.

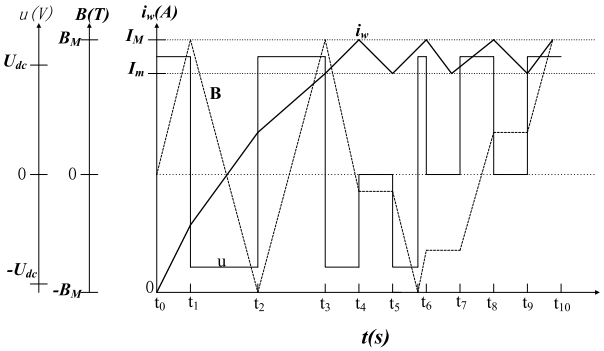

FIGURE 6. Schematic of the algorithm of the hysteresis control [44].

III. THREE-PHASE MEDIUM FREQUENCY DC RSW MACHINE

On the other hand, for three-phase medium frequency DC RSW machine, which has more complex structure when compared to single-phase AC RSW machine, the control action is to set each duty cycle of the PWM wave. Klopčič *et al.* [43] analyzed this structure, and pointed out that because the control frequency is very high and the structure may not exactly symmetrical, the magnetic saturation in the iron core of the welding transformer must be avoided, otherwise, the large current spikes may appear, which can activate over-current protection causing an unwanted switch-off of the spot welding system. Then they proposed a new advanced hysteresis control to replace the classical PWM voltage with closed-loop control of the welding current to reduce the current spikes and eliminate the magnetic saturation [44]. It included both of a closed-loop control of the welding current and a closed-loop control of the iron core saturation level in the welding transformer. The method required measuring the flux density B and the welding current i_w, and then through adjusting the output voltage of H-bridge to make B within the bounds $[-B_M, B_M]$, in the meanwhile, through switching on or off the supply voltage to make the i_w within the bounds $[-I_M, I_M]$. The schematic of the algorithm is shown in Figure.6 [44].

This method can avoid the appearance of magnetic saturation, and the actual output welding current approached a constant value. The method was tested through numerical analysis and actual experiments, the results showed that it can provide many advantages in comparison to the classical control of RSW system with the same structure. Also, in our previous work [45], the mathematical model of the three-phase medium frequency DC RSW was established in detail, then the magnetic and electrical characteristics was seriously explored. Then the work found that there was a dead zone of control action which may deteriorate the accuracy of welding current control. The problem can be solved through predicting the current variation tendency and adjust the duty cycle of PWM wave in advance, final simulation result validated the effectiveness of the method.

In addition, the welding transformer was usually mounted on the arm of moving robot, so the weight should be seriously considered in the design. Brezovnik *et al.* [46] analyzed the relation between the weight of the welding transformer and switching frequency, and then concluded that increasing the PWM switching frequency can reduce the weight the welding transformer, because the small iron core cross-section with a lighter core, and shorter and lighter windings were required. However, the high frequency may influence the maximum value of the welding current under the same load because the leakage inductance can affect the rise time of the primary current. The work presented an analytical solution which can directly calculate the maximum welding current in the steady state, and the equations allowed the calculations of the maximum welding current as a function of the other relative parameters. The model was confirmed by actual experimental measurement and numerical simulations using mathematical tools.

Also, the characteristic of the welding current in three-phase medium frequency DC RSW machine is shown in Figure.6. The waveform of welding current is so different when compared to that of single-phase AC RSW machine. The waveform is approximated to a DC curve, rather than discontinuous segments as shown in Figure.3 (b). Hence, the welding current passes through the parent metal sheets all the time. Through adjusting the PWM waves, the welding current can be within a narrow range during the whole welding duration [45]. In addition, it is easy to see that the control frequency of three-phase medium frequency DC RSW machine is much larger than that of single-phase AC RSW machine, so it has more opportunities to adjust the welding current to achieve a preliminary goal. Hence, the goal of CCC can be more smoothly achieved than that of single-phase AC RSW machine.

Furthermore, though the current control in three-phase medium frequency DC RSW machines can obtain more accurate result than that of single-phase AC RSW machine, previous work wanted to optimize the control process and achieve various types of current waveform effectively. Lee and Yu [47] used the fuzzy PI controller to improve the performance of the current waveform control of the machine.

The work used system identification method to model the PWM input and current waveform output system. The fuzzy scaling factors were optimized using a genetic algorithm. The results showed that the tracking effect was satisfactory no matter in the constant current waveform or arbitrary current waveforms. The work obtained significant improvements and experiences in the current control in the RSW machines with this type of electrical structure.

According to review works in this section, three-phase medium frequency DC RSW machine has a superior performance when compared to that of single-phase AC RSW machine. The power factor of three-phase medium frequency DC RSW machine approaches 100%, and it is easy to achieve the control goal, such as constant current control, because the control frequency is very high. Moreover, the efficiency of DC RSW is much higher than that of AC RSW machine, it may save 10% energy to obtain the nugget with the same size, according to some previous contributions [6], [48]. Also, the medium frequency DC RSW machine was more efficient in generating heat no matter in coated sheets or uncoated steels [49], [50]. However, the three three-phase medium frequency DC RSW machine has a more sophisticated structure, which can induce many negative phenomena. For example, frequently switching the positive and negative currents may induce magnetic saturation or current spike during the process. This is why many works about three-phase medium frequency DC RSW machine considered the welding transformer relative issues. In the future, many works are still required to improve the performance of three-phase medium frequency DC RSW machine, because the current model is much simpler with unsatisfied accuracy, and the equilibrium between effectiveness of energy delivery and magnetic stability is expected to be more improved.

IV. CONCLUSION

The recent advances of the applications of electrical structure in resistance spot welding has been reviewed in this paper. There are two types of RSW machines, which are single-phase AC RSW and medium frequency DC RSW machines. They have different energy delivery modes. Former type has a lower cost and simper structure but lower power factor, and the energy is not continuously supplied. The latter type can continuously supply energy, but has higher cost and more complex structure. Both two types have only one controllable input parameter, respectively the firing angle of SCR and duty cycle of the PWM wave. In other words, combined the characteristics of RSW operation, no matter which electrical structure is used, the systems are single-input-single-out (SISO). Some measures were taken to improve the performance of the machines, such as measure the welding current and power factor, design constant current controller and online measurement of dynamic resistance in single-phase AC RSW, or avoid magnetic saturation in medium frequency DC RSW.

Though the three-phase medium frequency DC RSW machine has more advantages, the relative work was less than that of single-phase AC RSW. The main reason is that the cost of the type of RSW machine is higher, and for many actual application, the RSW machine with single-phase AC power source can meet the requirement. Under the current circumstance, the two types of RSW machines have their special applied occasions. Hence, both two types should be seriously concerned in reality, no matter in academic research or actual industrial production. In the future, it is expected that the research of the electrical structure is collaborative to the process analysis, process control of the RSW operations, and then realize the more general operational strategies, at the same time eliminate the negative phenomena.

REFERENCES

[1] R. W. Messler, Jr., and M. Jou, "Review of control systems for resistance spot welding: Past and current practices and emerging trends," *Sci. Technol. Welding Joining*, vol. 1, no. 1, pp. 1–9, 1996.
[2] Ó. Marín, P. De Tiedra, and M. San-Juan, "Combined effect of resistance spot welding and precipitation hardening on tensile shear load bearing capacity of A286 superalloy," *Mater. Sci. Eng. A*, vol. 688, pp. 309–314, Mar. 2017.
[3] J. Bi, J. Song, Q. Wei, Y. Zhang, Y. Li, and Z. Luo, "Characteristics of shunting in resistance spot welding for dissimilar unequal-thickness aluminum alloys under large thickness ratio," *Mater. Des.*, vol. 101, pp. 226–235, Jul. 2016.
[4] M. Pouranvari and S. P. H. Marashi, "Critical review of automotive steels spot welding: Process, structure and properties," *Sci. Technol. Welding Joining*, vol. 18, no. 5, pp. 361–403, 2013.
[5] Y. Li, Z. Lin, Q. Shen, and X. Lai, "Numerical analysis of transport phenomena in resistance spot welding process," *J. Manuf. Sci. Eng.*, vol. 133, no. 3, pp. 031019-1–031019-8, 2011.
[6] W. Li, D. Cerjanec, and G. A. Grzadzinski, "A comparative study of single-phase AC and multiphase DC resistance spot welding," *J. Manuf. Sci. Eng.*, vol. 127, no. 3, pp. 583–589, 2005.
[7] S. C. A. Alfaro, J. E. Vargas, M. A. Wolff, and L. O. Vilarinho, "Comparison between AC and MF-DC resistance spot welding by using high speed filming," *J. Achievements Mater. Manuf. Eng.*, vol. 24, no. 1, pp. 333–339, 2007.
[8] J. Yu, "New methods of resistance spot welding using reference waveforms of welding power," *Int. J. Precis. Eng. Manuf.*, vol. 17, no. 10, pp. 1313–1321, 2016.
[9] P. Podržaj, I. Polajnar, J. Diaci, and Z. Kariž, "Overview of resistance spot welding control," *Sci. Technol. Welding Joining*, vol. 13, no. 3, pp. 215–224, 2008.
[10] K. Zhou and L. Cai, "Online measuring power factor in AC resistance spot welding," *IEEE Trans. Ind. Electron.*, vol. 61, no. 1, pp. 575–582, Jan. 2014.
[11] W. Li, E. Feng, D. Cerjanec, and G. A. Grzadzinski, "Energy consumption in AC and MFDC resistance spot welding," presented at the Proc. 11th Sheet Metal Welding Conf., Sterling Heights, MI, USA, 2004.
[12] D. C. Kim, H. J. Park, I. S. Hwang, and M. J. Kang, "Resistance spot welding of aluminum alloy sheet 5J32 using SCR type and inverter type power supplies," *Arch. Mater. Sci. Eng.*, vol. 38, no. 1, pp. 55–60, 2009.
[13] M. Matsushita, R. Ikeda, and K. Oi, "Development of a new program control setting of welding current and electrode force for single-side resistance spot welding," *Welding World*, vol. 59, no. 4, pp. 533–543, 2015.
[14] M. Matsushita, R. Ikeda, and K. Oi, "Development of in-process welding current and electrode force control process for single-side resistance spot welding," JFE, Tokyo, Japan, Tech. Rep. 20, 2015, pp. 92–98.
[15] C.-P. Liang, Z.-Q. Lin, G.-L. Chen, and Y.-B. Li, "Numerical analysis of single sided spot welding process used in sheet to tube joining," *Sci. Technol. Welding Joining*, vol. 11, no. 5, pp. 609–617, 2006.
[16] B. H. Chang, M. V. Li, and Y. Zhou, "Comparative study of small scale and 'large scale' resistance spot welding," *Sci. Technol. Welding Joining*, vol. 6, no. 5, pp. 273–280, 2001.
[17] J. Chen, D. F. Farson, K. Ely, and T. Frech, "Modeling small-scale resistance spot welding machine dynamics for process control," *Int. J. Adv. Manuf. Technol.*, vol. 27, nos. 7–8, pp. 672–676, 2006.

[18] T. C. Manjunath, S. Janardhanan, and N. S. Kubal, "Simulation, design, implementation and control of a welding process using micro-controller," in *Proc. 5th Asian Control Conf.*, Jul. 2004, pp. 828–836.

[19] X. C. Wang and M. Y. Lui, "An arbitrary waveform control system for a precise spot-welding power source," *J. Mater. Process. Technol.*, vol. 122, nos. 2–3, pp. 185–188, 2002.

[20] K. Zhou and L. Cai, "A nonlinear current control method for resistance spot welding," *IEEE/ASME Trans. Mechatronics*, vol. 19, no. 2, pp. 559–569, Apr. 2014.

[21] S. Dhandapani, M. Bridges, and E. Kannatey-Asibu, "Nonlinear electrical modeling for the resistance spot welding process," in *Proc. Amer. Control Conf.*, Jun. 1999, pp. 182–186.

[22] K. Zhou and L. Cai, "Study of safety operation of AC resistance spot welding system," *IET Power Electron.*, vol. 7, no. 1, pp. 141–147, Jan. 2014.

[23] L. Gong, C.-L. Liu, and X. F. Zha, "Model-based real-time dynamic power factor measurement in AC resistance spot welding with an embedded ANN," *IEEE Trans. Ind. Electron.*, vol. 54, no. 3, pp. 1442–1448, Jun. 2007.

[24] T. L. Baldwin, T. Hogans, Jr., S. D. Henry, F. Renovich, Jr., and P. T. Latkovic, "Reactive-power compensation for voltage control at resistance welders," *IEEE Trans. Ind. Appl.*, vol. 41, no. 6, pp. 1485–1492, Nov. 2005.

[25] W.-H. Ko and J.-C. Gu, "Design and application of a thyristor switched capacitor bank for a high harmonic distortion and fast changing single-phase electric welding machine," *IET Power Electron.*, vol. 9, no. 15, pp. 2751–2759, Dec. 2016.

[26] P. Podržaj, I. Polajnar, J. Diaci, and Z. Karič, "Influence of welding current shape on expulsion and weld strength of resistance spot welds," *Sci. Technol. Welding Joining*, vol. 11, no. 3, pp. 250–254, 2006.

[27] S. Gao, L. Budde, and L. Wu, "Investigation of the effective welding current in spot welding," in *Proc. ASME Winter Annu. Meet., Prod. Eng. Division*, 1993, pp. 965–970.

[28] L. Gong, C.-L. Liu, and L. Guo, "Residual adaptive algorithm applied in intelligent real-time calculation of current RMS value during resistance spot welding," in *Proc. Int. Conf. Neural Netw. Brain (ICNN&B)*, Oct. 2005, pp. 1800–1806.

[29] K. Zhou and L. Cai, "An algorithm for calculating the RMS value of the non-sinusoidal current used in AC resistance spot welding," *J. Power Electron.*, vol. 15, no. 4, pp. 1139–1147, 2015.

[30] S. Aslanlar, "The effect of nucleus size on mechanical properties in electrical resistance spot welding of sheets used in automotive industry," *Mater. Des.*, vol. 27, no. 2, pp. 125–131, 2006.

[31] K. Zhou, "Development of an online quality control system for resistance spot welding," Ph.D. dissertation, Dept. Mech. Eng., Hong Kong Univ. Sci. Technol., Hong Kong, 2013.

[32] M. El-Banna, D. Filev, and R. B. Chinnam, "Online qualitative nugget classification by using a linear vector quantization neural network for resistance spot welding," *Int. J. Adv. Manuf. Technol.*, vol. 36, nos. 3–4, pp. 237–248, Mar. 2008.

[33] K. Zhou and L. Cai, "Online nugget diameter control system for resistance spot welding," *Int. J. Adv. Manuf. Technol.*, vol. 68, nos. 9–12, pp. 2571–2588, 2013.

[34] X. Zhao and L. Cai, "Current control for single phase AC resistance spot welding systems using Fourier learning scheme," in *Proc. 26th IASTED Int. Conf. Modelling, Identificat., Control (MIC)*, 2007, pp. 7–12.

[35] K. Zhou, P. Yao, and L. Cai, "Constant current vs. constant power control in AC resistance spot welding," *J. Mater. Process. Technol.*, vol. 223, pp. 299–304, Sep. 2015.

[36] D. W. Adams, C. D. E. Summerville, B. M. Voss, J. Jeswiet, and M. C. Doolan, "Correlating variations in the dynamic resistance signature to weld strength in resistance spot welding using principal component analysis," *J. Manuf. Sci. Eng.*, vol. 139, no. 4, pp. 044502-1–044502-4, 2007.

[37] S. A. Gedeon, C. D. Sorensen, K. T. Ulrich, and T. W. Eagar, "Measurement of dynamic electrical and mechanical properties of resistance spot welds," *Welding J.*, vol. 66, no. 2, pp. 378s–385s, 1987.

[38] X. Chen and K. Araki, "Fuzzy adaptive process control of resistance spot welding with a current reference model," in *Proc. IEEE Int. Conf. Intell. Process. Syst.*, Oct. 1997, pp. 190–194.

[39] Y. Cho and S. Rhee, "New technology for measuring dynamic resistance and estimating strength in resistance spot welding," *Meas. Sci. Technol.*, vol. 11, no. 8, pp. 1173–1178, Aug. 2000.

[40] Y. Cho and S. Rhee, "Primary circuit dynamic resistance monitoring and its application to quality estimation during resistance spot welding," *Welding J.*, vol. 81, no. 6, pp. 104s–111s, 2002.

[41] J. D. Cullen *et al.*, "Multisensor fusion for on line monitoring of the quality of spot welding in automotive industry," *Measurement*, vol. 41, no. 4, pp. 412–423, 2008.

[42] Y. Luo, W. Rui, X. Xie, and Y. Zhu, "Study on the nugget growth in single-phase AC resistance spot welding based on the calculation of dynamic resistance," *J. Mater. Process. Technol.*, vol. 229, pp. 492–500, Mar. 2016.

[43] B. Klopčič, D. Dolinar, and G. Štumberger, "Analysis of an inverter-supplied multi-winding transformer with a full-wave rectifier at the output," *J. Magn. Magn. Mater.*, vol. 320, no. 20, pp. e929–e934, 2008.

[44] B. Klopčič, D. Dolinar, and G. Štumberger, "Advanced control of a resistance spot welding system," *IEEE Trans. Power Electron.*, vol. 23, no. 1, pp. 144–152, Jan. 2008.

[45] K. Zhou and L. Cai, "Improvement in control system for the medium frequency direct current resistance spot welding system," in *Proc. Amer. Control Conf.*, San Francisco, CA, USA, Jun./Jul. 2011, pp. 2657–2662.

[46] R. Brezovnik, J. Černelič, M. Petrun, D. Dolinar, and J. Ritonja, "Impact of the switching frequency on the welding current of a spot-welding system," *IEEE Trans. Ind. Electron.*, vol. 64, no. 12, pp. 9291–9301, Dec. 2017.

[47] H. Lee and J. Yu, "Development of fuzzy controller for inverter DC resistance spot welding using system identification," *J. Mech. Sci. Technol.*, vol. 31, no. 8, p. 3961 3968, 2017.

[48] D. Venugopal, M. Das, and V. Fernandez, "Study and implementation of a force stepper and a part fit-up solver algorithm for a servo controlled MFDC spot welder," in *Proc. IEEE Int. Conf. Electro/Inf. Technol. (EIT)*, Jun. 2009, pp. 286–291.

[49] M. Batista and S. D. Brandi, "Use of dynamic resistance and dynamic energy to compare two resistance spot welding equipments for automotive industry in zinc coated and uncoated sheets," *Amer. J. Eng. Res.*, vol. 2, no. 6, pp. 79–93, 2013.

[50] J. Černelič, R. Brezovnik, J. Ritonja, D. Dolinar, and M. Petrun, "Optimal operating point of medium frequency resistance spot welding systems," in *Proc. IEEE 26th Int. Symp. Ind. Electron. (ISIE)*, Edinburgh, U.K., Jun. 2017, pp. 2131–2137.

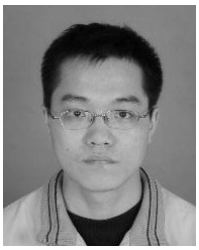

KANG ZHOU received the bachelor's and master's degrees from the School of Automation, Northwestern Polytechnical University, Xi'an, China, in 2005 and 2008, respectively, and the Ph.D. degree from the Department of Mechanical Engineering, The Hong Kong University of Science and Technology, Hong Kong, in 2013. He is currently an Associate Professor with the Institute of Mechanics, Chinese Academy of Sciences. His research interests are in electrical engineering, mechatronics, and intelligent control of welding systems.

PING YAO received the bachelor's and master's degrees from Central South University, Changsha, China, and the Ph.D. degree from the South China University of Technology, Guangzhou, China. She is currently a Professor and an Associate Dean of the College of Electromechanical Engineering, Guangdong Polytechnic Normal University, Guangzhou. She is also the Director of the research center of industrial robotics intelligent driving system and application engineering. Her research interests focus on industrial robotics and intelligent equipments, intelligent monitoring and control in the manufacturing process, signal processing, and structural health monitoring. She received many awards, including the Science and Technology Award of Guangdong.